

# Sensory Organ Remodeling in *Caenorhabditis elegans* Requires the Zinc-Finger Protein ZTF-16

Carl Procko, Yun Lu, and Shai Shaham<sup>1</sup>

Laboratory of Developmental Genetics, The Rockefeller University, New York, New York 10065

**ABSTRACT** Neurons and glia display remarkable morphological plasticity, and remodeling of glia may facilitate neuronal shape changes. The molecular basis and control of glial shape changes is not well understood. In response to environmental stress, the nematode *Caenorhabditis elegans* enters an alternative developmental state, called dauer, in which glia and neurons of the amphid sensory organ remodel. Here, we describe a genetic screen aimed at identifying genes required for amphid glia remodeling. We previously demonstrated that remodeling requires the Otx-type transcription factor TTX-1 and its direct target, the receptor tyrosine kinase gene *ver-1*. We now find that the *hunchback/Ikaros*-like C2H2 zinc-finger factor *ztf-16* is also required. We show that *ztf-16* mutants exhibit pronounced remodeling defects, which are explained, at least in part, by defects in the expression of *ver-1*. Expression and cell-specific rescue studies suggest that *ztf-16*, like *ttx-1*, functions within glia; however, promoter deletion studies show that *ztf-16* acts through a site on the *ver-1* promoter that is independent of *ttx-1*. Our studies identify an important component of glia remodeling and suggest that transcriptional changes may underlie glial morphological plasticity in the sensory organs of *C. elegans*.

THE shapes of neuronal receptive structures such as dendritic spines and sensory receptive endings are plastic and can be remodeled by developmental, hormonal, and environmental signals. For example, the dendritic spines of Purkinje cells rapidly grow and retract during development of the mouse cerebellum (Dunaevsky *et al.* 1999), and estrogen levels affect the number and density of dendritic spines in the hippocampus during the estrous cycle in rats (Woolley *et al.* 1990). In the mouse barrel cortex, changes in somatosensory environmental input increase the turnover of pyramidal neuron dendritic spines (Trachtenberg *et al.* 2002). Likewise, reduced sensory input affects the shape of the AWB neuron sensory ending in the nematode *Caenorhabditis elegans* (Mukhopadhyay *et al.* 2008).

Glia, which are intimately associated with neurons, also exhibit complex shapes and morphological plasticity, and changes in glial shape often correlate with neuronal remodeling (Procko and Shaham 2010). For example, retraction of astrocyte processes in the hypothalamus of lactating rats cor-

relates with synaptic changes in associated supraoptic nucleus neurons (Theodosis and Poulain 1993); and perturbation of the glial ephrin-A3 cell-surface protein affects the shape of dendritic spines in the mouse hippocampus (Carmona *et al.* 2009). These observations, coupled with the close proximity of glia to neurons and the ability of glia to regulate and perceive their extracellular environment (Meyer-Franke *et al.* 1995; Porter and McCarthy 1996), suggest that glia are well positioned to facilitate or, more speculatively, to direct changes in neuronal receptive ending shapes. Although glial shape changes in vertebrate systems have been documented (Theodosis and Poulain 1993; Lippman *et al.* 2008), the molecular basis for these changes is not well understood.

The nematode *C. elegans* has a relatively small number of glia and neurons with stereotyped shapes (Ward *et al.* 1975; White *et al.* 1986), and, unlike vertebrate glia, *C. elegans* glia can be ablated without affecting neuronal survival (Bacaj *et al.* 2008; Yoshimura *et al.* 2008). In response to environmental stressors, including starvation, crowding, and high temperature, *C. elegans* enters a developmentally arrested stress-resistant state termed “dauer” (Cassada and Russell 1975; Golden and Riddle 1984), in which the anterior bilateral amphid sensory organs are remodeled (Albert and Riddle 1983). Each amphid consists of sensory neurons that extend dendritic processes to the nose tip and there terminate in specialized sensory endings. Associated with these neurons are single amphid sheath

Copyright © 2012 by the Genetics Society of America  
doi: 10.1534/genetics.111.137786

Manuscript received December 13, 2011; accepted for publication January 20, 2012  
Available freely online through the author-supported open access option.

Supporting information is available online at <http://www.genetics.org/content/suppl/2012/01/31/genetics.111.137786.DC1>.

<sup>1</sup>Corresponding author: 1031 Weiss Research Bldg., The Rockefeller University, 1230 York Avenue, New York, NY 10065. E-mail: shaham@rockefeller.edu

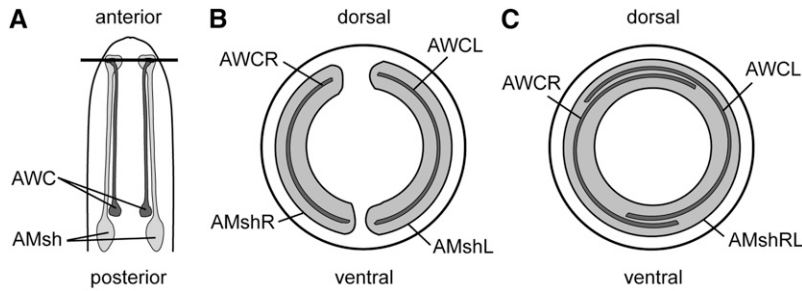


**Figure 1** A schematic of amphid sensory organ remodeling in *C. elegans* dauer animals. (A) A schematic of the head of the animal, showing the two bilateral AMsh glia and AWC sensory neurons. The horizontal line indicates the position of the transverse sections shown in B and C. (B and C) Sections through the nose tip showing the left and right AWC neuron receptive endings (AWCL/R; dark shading) and the ensheathing AMsh glia (AMshL/R; light shading) in wild-type non-dauer (B) and dauer (C) animals. Note AMsh glial fusion and AWC receptive ending expansion and overlap in dauers.

(AMsh) glial cells. Each AMsh glia also extends a process toward the nose tip, and there ensheaths sensory neuron ciliated receptive endings (Figure 1A) (Ward *et al.* 1975). In dauer animals, the two AMsh glia expand at the nose tip and use the protein AFF-1 to fuse (Albert and Riddle 1983; Procko *et al.* 2011). Concomitantly, the ciliated sensory endings of the AWC amphid neurons expand within the new compartment defined by the glia, such that the left and right AWC cilia now extensively overlap (Figure 1, B and C). Importantly, AMsh glia remodel even in the absence of the AWC neurons, and blocking glial remodeling perturbs AWC neuron shape, suggesting that glial remodeling facilitates neuronal shape changes (Procko *et al.* 2011).

We previously found that glial remodeling depends on the *Otx*-type transcription factor *ttx-1* and its direct target gene, the receptor tyrosine kinase *ver-1*, both acting within AMsh glia (Procko *et al.* 2011). Expression of *ver-1* is induced in AMsh glia following dauer entry and in non-dauer animals of all stages upon cultivation at high temperature (25°), a dauer stimulus. Here, we report results of a genetic screen aimed at identifying mutants defective in *ver-1* expression and identify the gene *ztf-16* (zinc-finger putative transcription factor family) as a major regulator of *ver-1* expression and AMsh glia remodeling. Our results suggest that transcription factors play important roles in AMsh glia morphological plasticity.

## Materials and Methods

### Strains

Animals were cultivated at 20° using standard methods (Brenner 1974), unless otherwise noted. The wild-type strain used was Bristol (N2). Mutant alleles used were the following: LGIII—*daf-7(e1372)* and *lit-1(ns132, t1512)*; and LGV—*ttx-1(p767, oy26)*. Mutant alleles isolated in this study were the following: LGV—*tam-1(ns167, ns170, ns174, ns234, ns237, ns238, ns241, ns249, ns258, ns268)* and *ttx-1(ns235, ns252, ns255, ns259, ns260, ns267)*; and LGX—*ztf-16(ns169, ns171, ns178)*. Alleles not mapped to a chromosome include *ns231* and *ns257*. *ver-1* promoter::*gfp* was *nsIs22*. Other integrated transgenes and extrachromosomal arrays are as indicated elsewhere in the text.

### Plasmid construction and isolation of cDNAs

The initial *ver-1* promoter::*gfp* construct (~2 kb upstream promoter through +263 of the *ver-1* gene fused to *gfp*) was a gift

of R. Roubin and C. Popovici. Vector backbones are derived from the pPD vectors (gift of A. Fire). cDNA template was prepared from mixed-stage animals. The glia::*ztf-16a* and glia::*ztf-16b* constructs were made by replacing the heat-shock promoter of vector pPD49.78 with a 2-kb promoter from the *F16F9.3* gene (Bacaj *et al.* 2008) at *PstI/BamHI* and then inserting either *ztf-16a* or *ztf-16b* cDNA at *XmaI/NcoI*. The glia::*ztf-16* construct that was integrated to generate strain *nsIs245* was made by inserting 2.5 kb of the *T02B11.3* promoter (Bacaj *et al.* 2008) into pPD49.78 at *PstI/BamHI* and *ztf-16b* cDNA at *XmaI/SacI*. Embryonic glia::*ztf-16b* was made by inserting a *lin-26* glia enhancer region and a *myo-2* minimal promoter (Landmann *et al.* 2004) into pPD49.78 at *SphI/XmaI*, followed by *ztf-16b* at *XmaI/NcoI*. The *F16F9.3* promoter was inserted into the *PstI* site of pPD95.75 followed by *ztf-16b* cDNA in frame with *gfp* at *XmaI/KpnI* to generate glia promoter::*ztf-16b*::*gfp*. The *ztf-16* promoter::*gfp* construct that gave *gfp* expression in the amphid and phasmid glia included the region -4637 to -2536 of the *ztf-16* promoter relative to the +1 translation start site inserted into pPD95.75 at *SphI/KpnI*. To generate the *F58F9.10* promoter::*gfp* construct, 2 kb of upstream promoter was inserted into pPD95.75 at *SphI/BamHI*. To make the *F58F9.6* promoter::*gfp*, a 4-kb *BamHI/XmaI* promoter fragment was inserted at *BamHI/AgeI*.

### Germline transformation and transgene integration

Germline transformations were carried out using standard protocols (Mello and Fire 1995). Co-injection markers used were either plasmid pRF4 (Mello *et al.* 1991) or *unc-122* promoter::*dsRed*. pSL1180 (GE Healthcare) is an empty cloning vector used to increase the DNA concentration of injection mixtures. The glia promoter::*ztf-16* rescue transgene (*nsIs245*) was integrated by treating animals carrying extrachromosomal arrays with UV/psoralen (Mello and Fire 1995). The generated strain was backcrossed to N2 three times.

### Microscopy

*ver-1* promoter::*gfp* (*nsIs22*) expression was assayed using a fluorescence dissecting microscope (Leica). Adult hermaphrodites were scored, except as noted. Compound microscope images were taken on an Axioplan II microscope using an AxioCam CCD camera (Zeiss) and analyzed using Axiovision software (Zeiss). Additional images were taken on a Deltavision Image Restoration Microscope (Applied Precision/Olympus) and analyzed using SoftWoRx software (Applied Precision). Dauer animals for electron microscopy

(EM) were grown at 25°. These were prepared and sectioned using standard methods (Lundquist *et al.* 2001). Imaging was performed with an FEI Tecnai G2 Spirit BioTwin transmission electron microscope equipped with a Gatan 4K × 4K digital camera.

### **Dauer selection**

Animals were starved and dauers selected by treatment with 1% SDS in M9 solution for 20 min. Alternatively, animals carrying the *daf-7(e1372)* mutation were induced to form dauers by incubation at 25°.

### **Mutagenesis and mapping**

L4 animals carrying the *ver-1* promoter::*gfp* transgene (*nsIs22*) in the N2 strain background were mutagenized with 30 mM ethyl methanesulfonate (EMS) for 4 hr. Mutagenized animals were picked to separate 9-cm NGM agar plates seeded with *Escherichia coli* OP50 and cultivated at 25°. F<sub>2</sub> animals were screened. Mapping was performed by crossing to the Hawaiian strain (CB4856), picking mutant F<sub>2</sub> progeny, and observing linkage to single nucleotide polymorphisms (SNPs) (Wicks *et al.* 2001).

### **Cytoplasmic mixing assay to score AMsh glia fusion**

Adult animals carrying an *nsEx1391* (AMsh glia::*gfp*) array were picked to plates seeded with OP50 bacteria and cultivated at 25°. From these plates, L1 and L2 progeny carrying the *nsEx1391* array in one of the two AMsh glia were picked to freshly seeded plates. These mosaic animals were incubated for 48 hr at 25° before scoring GFP presence in either one or both AMsh glia. Animals carrying a *daf-7(e1372)* mutation were scored only if they were dauer larvae by morphology at the end of the assay period. See Procko *et al.* (2011).

### **Behavioral assays**

Thermotaxis and chemotaxis assays were performed as previously described (Procko *et al.* 2011).

## **Results**

### **A genetic screen for mutants defective in *ver-1* expression**

To study how dauer remodeling is initiated, we aimed to identify mutants defective in this process. However, existing methodologies for following the remodeling process—namely electron microscopy and assessment of glial fusion by tracking mosaic animals (Procko *et al.* 2011)—are low throughput. We turned, therefore, to a more indirect approach. The *C. elegans* tyrosine-kinase receptor gene *ver-1* is expressed in the AMsh and phasmid sheath (PHsh) glia of the amphid and phasmid sensory organs upon dauer entry and at high temperature (25°) and is important for amphid glia remodeling in dauers. *ver-1* induction in dauers and at high temperature is, at least in part, similarly regulated as mutations in *ttx-1*, encoding a direct transcriptional activator of *ver-1*, blocks induction in both settings (Procko *et al.* 2011). Fur-

thermore, *ttx-1* mutations also block AMsh glia remodeling in dauers. To identify genes involved in the initiation of glia remodeling, we therefore sought mutants with defects in *ver-1* expression at high temperature. Wild-type animals carrying a *ver-1* promoter::*gfp* reporter transgene (*nsIs22*) were mutagenized with EMS, and >35,000 F<sub>2</sub> progeny grown at 25° were screened for reduced GFP fluorescence in AMsh glia. A total of 21 independent mutant alleles were identified (Table 1). Two of these alleles, *ns235* and *ns252*, failed to complement the *ttx-1(p767)* allele when scored for *ver-1* promoter::*gfp* expression (Table 1), and both had the same G-to-A nucleotide change within the *ttx-1*-coding region, altering amino acid 230 from glutamate to lysine (Figure 2). The isolation of mutations in *ttx-1*, a known glial remodeling regulator, validated our screen strategy.

Four of the mutant lines that we identified, *ns255*, *ns259*, *ns260*, and *ns267*, had a strong dominant reduction in *ver-1* promoter::*gfp* expression and could not be assayed in complementation studies (Table 1; data not shown). As shown in Figure 2 and in Supporting Information, Figure S1, all four dominant alleles also had sequence changes within the *ttx-1*-coding region. The allele *ns260*, which is predicted to lack sequences encoding the TTX-1 DNA-binding domain, is likely homozygous embryonic lethal, as viable progeny from *ns260/+* parents either were homozygous for the wild-type *ttx-1* allele and expressed wild-type levels of *ver-1* promoter::*gfp* or were *ns260/+* and had low GFP fluorescence (Figure S2A). Consistent with an essential role for *ttx-1*, we found that animals heterozygous for the dominant *ttx-1* allele *ns259* also gave rise to fewer than expected *ns259* homozygous progeny. Only 7 of 68 progeny of an *ns259/+* parent grown at 25° were *ns259* homozygotes ( $P = 0.02$ ,  $\chi^2$  test), and all 7 homozygotes were sterile. Similarly, at 15°, 6 of 65 progeny were *ns259* homozygotes ( $P < 0.02$ ), and all were sterile.

*ttx-1* is expressed in both AMsh glia and the AFD thermosensory neurons (Satterlee *et al.* 2001; Procko *et al.* 2011). However, we were unable to rescue *ttx-1(ns260)* lethality using either glial or AFD promoters (Figure S2). In addition, sterile *ns259* homozygous animals possessed AMsh glia of normal morphology, as assayed by expression of a glial *F16F9.3* promoter::*dsRed* transgene ( $n = 16$ ). Taken together, these results suggest that *ttx-1* is likely to have essential developmental roles in cells other than AMsh glia and the AFD neuron.

Nine of the alleles that we isolated failed to complement the allele *ns258*, also identified in our screen (Table 1; data not shown). SNP mapping (Wicks *et al.* 2001) was used to map one of these alleles, *ns268*, to a ~160-kb interval on chromosome V (Figure 3A). Cosmid F26G5 within this interval rescued the *ver-1* expression defect when injected into *ns268* mutants (Figure 3B), and sequencing of coding regions spanned by this cosmid uncovered two mutations within the gene *tam-1*. Mutations in *tam-1* were also identified in each of the other nine alleles of this complementation group (Figure 3C), confirming *tam-1* as the relevant affected gene. *tam-1* encodes a protein predicted to contain a C3HC4 zinc finger (RING finger) and a B-box motif and has been shown to

**Table 1 Mutant strains that reduce *ver-1* promoter::*gfp* expression**

Allele <sup>a</sup>	<i>ver-1</i> expression 25 <sup>o</sup> <sup>a</sup>	
	% AMsh on	<i>n</i>
Wild type	98	60
Complementation group 1 (see also dominant alleles below)		
<i>ttx-1</i> (p767) (reference allele) <sup>b</sup>	0	40
<i>ns235</i>	0	64
<i>ns252</i>	0	62
Complementation group 2		
<i>ns258</i> (reference allele) <sup>b</sup>	6	52
<i>ns167</i>	72 <sup>c</sup>	54
<i>ns170</i>	17	54
<i>ns174</i>	5	44
<i>ns234</i>	16	55
<i>ns237</i>	69 <sup>c</sup>	51
<i>ns238</i>	4	45
<i>ns241</i>	31	52
<i>ns249</i>	2	45
<i>ns268</i>	45	60
Complementation group 3		
<i>ns171</i> (reference allele) <sup>b</sup>	4	55
<i>ns169</i>	14	51
<i>ns178</i>	2	52
Alleles not falling into complementation groups 1–3		
<i>ns231</i>	48 <sup>c</sup>	52
<i>ns257</i>	70 <sup>c</sup>	50
Dominant alleles <sup>d</sup>		
<i>ns255</i> <sup>e</sup>	0	42
<i>ns259</i> / <sup>f</sup>	2	44
<i>ns260</i> / <sup>f</sup>	42	84
<i>ns267</i>	0	40

<sup>a</sup> All strains contained the *ver-1* promoter::*gfp* transgene (*ns122*).

<sup>b</sup> The reference alleles were used to place other alleles into complementation groups.

<sup>c</sup> These alleles mostly had weak, qualitative effects on *ver-1* promoter::*gfp* expression.

<sup>d</sup> Dominant alleles were not scored for complementation. All dominant alleles were found to have a mutation in the *ttx-1* gene.

<sup>e</sup> Animals homozygous for allele *ns255* were slow growing and unhealthy.

<sup>f</sup> Alleles *ns259* and *ns260* were homozygous sterile and lethal, respectively. These strains were isolated from the screen as heterozygotes and are scored as such. Of the *ns260*/<sup>f</sup> animals that expressed *ver-1* promoter::*gfp*, fluorescence was qualitatively reduced.

broadly and nonspecifically regulate gene expression of transgenes from simple DNA arrays (Hsieh *et al.* 1999). Therefore, the effects of *tam-1* mutations on *ver-1* promoter::*gfp* expression may not reflect a role in the control of endogenous *ver-1* expression, and we did not pursue further characterization of this gene.

Two additional alleles identified in our screen, *ns231* and *ns257*, did not harbor mutations in *ttx-1*, *tam-1*, or *ztf-16* (see below), had only weak defects in *ver-1* expression, and were not further studied.

### **C2H2 zinc-finger factor *ztf-16* is required for *ver-1* expression**

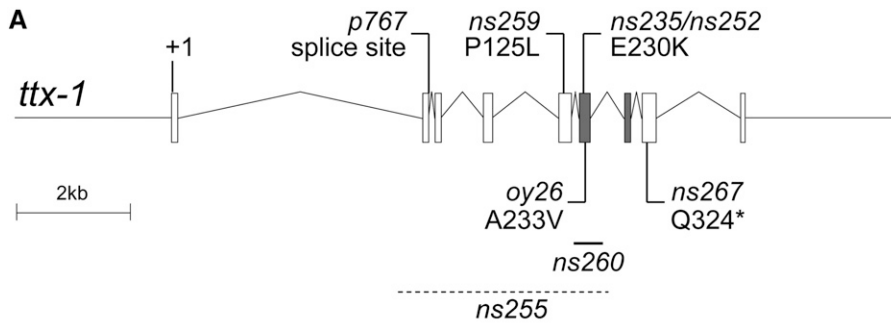
The *ns169* and *ns178* alleles fail to complement *ns171*, another allele isolated in our screen, and in all three alleles expression of a *ver-1* promoter::*gfp* transgene in the AMsh and PHsh glia of adult animals raised at 25° is strongly

attenuated (Table 1; Figure 4, A and B; data not shown). Furthermore, whereas 100% of wild-type dauers expressed *ver-1* promoter::*gfp* in the AMsh glia, 0% of *ns169*, *ns171*, or *ns178* mutant dauers induced by starvation at 15° expressed the reporter (*n* = 50 for each allele; Figure 4C). By contrast, mutations in this complementation group had little or no effect on an AMsh glia reporter that is expressed constitutively and independently of dauer entry (Figure 4D). Unlike mutations in *ttx-1*, which also disrupt AFD sensory neuron-mediated thermotaxis behavior and AFD morphology (Hedgecock and Russell 1975; Satterlee *et al.* 2001; Procko *et al.* 2011), *ns171* mutants exhibited nearly normal thermotaxis behavior and AFD morphology (Figure 5, A–F; Figure S3). Together, these observations suggest that the gene defined by the *ns171* complementation group is specifically required for *ver-1* promoter::*gfp* expression in AMsh glia and does not affect glial cell fate, AFD cell fate, or general aspects of gene expression in these cells.

To identify the gene corresponding to the *ns171* complementation group, we used SNP mapping (Wicks *et al.* 2001) to place the *ns171* mutation within an interval of ~370 kb on chromosome X (Figure 6A). Cosmids spanning the 5' region of this interval were injected into *ns171* mutants and scored for rescue of *ver-1* promoter::*gfp* expression in adults raised at 25°. One of these cosmids, R08E3, gave rescue (Figure 6B). Candidate coding regions were sequenced within this interval, and a single C-to-T substitution at codon 236 of the *ztf-16* open reading frame was identified. This mutation is predicted to cause a premature stop (Figure 6C). *ns178* mutants have the same base alteration as *ns171* animals, and *ns169* mutants harbor a different C-to-T mutation, at codon 131, which is also predicted to generate a premature stop (Figure 6C). Taken together, these studies demonstrate that *ztf-16* is the relevant gene affected in mutants of the *ns171* complementation group.

*ztf-16* encodes a protein predicted to contain up to eight C2H2 zinc-finger domains. C2H2 zinc-finger proteins are abundant transcriptional regulators in mammals, with >130 expressed in the brain alone (Iuchi 2001). On the basis of the pattern of C2H2 zinc fingers, *ztf-16* has been classified as a *hunchback*- and *Ikaros*-like transcription factor (Large and Mathies 2010). In vertebrates, the *Ikaros* family of C2H2 zinc-finger transcription factors have broad roles in the development of the hematopoietic system (Smale and Dorshkind 2006), while *hunchback* was identified as a factor regulating *Drosophila* embryo patterning (Tautz *et al.* 1987). *hunchback*- and *Ikaros*-like transcription factors have a unique arrangement of C2H2 zinc fingers: four amino-terminal or middle C2H2 zinc fingers bind DNA (Molnar and Georgopoulos 1994), while two carboxy-terminal C2H2 zinc fingers mediate dimerization (McCarty *et al.* 2003). In *ztf-16*, it is likely that zinc fingers 3–6 form the putative DNA-binding domain (Large and Mathies 2010).

On the basis of expressed sequence tag (EST) data available from WormBase (release WS225), we isolated two alternatively spliced cDNAs, *ztf-16a* and *ztf-16b*, derived from the *ztf-16* locus. ZTF-16a and ZTF-16b proteins are predicted to differ at their carboxy-termini. ZTF-16a lacks zinc fingers



**B**

		ns235/ns252
		E230K
TTX-1A (197)	RKQRRERTTFTRNQLLEISYFVKTRYPDIFMREDMAHKIQLPESRVQVWFKNRRAKARQQKKTLL	
OTD (71)	RKQRRERTTFTRAQLDVLLEALFGKTRYPDIFMREEVALKINLPESRVQVWFKNRRAKCRQQQLQQQ	
Otx1 (36)	RKQRRERTTFTRSQLDVLEALFAKTRYPDIFMREEVALKINLPESRVQVWFKNRRAKCRQQQSG	
Otx2 (36)	RKQRRERTTFTRAQLDVLLEALFAKTRYPDIFMREEVALKINLPESRVQVWFKNRRAKCRQQQSG	
	***** **::** * ***** _:.* *****	

(\*) conserved residue      (:) conserved substitution      (.) semi-conserved substitution

Alignment of the DNA-binding homeodomains of Otx-type factors TTX-1 (A isoform), *Drosophila* OTD, and murine Otx1 and Otx2. Amino acid positions are shown in parentheses. ns235 and ns252 (and ns255) code for a glutamic acid to lysine change in a conserved residue.

7 and 8, possessing instead a short sequence absent in ZTF-16b (Figure 6C).

### ztf-16 functions within glia to regulate ver-1 expression

*ztf-16* was previously suggested to play a minor role in somatic gonad development and was shown to be expressed in this tissue (Large and Mathies 2010). Our findings suggest that *ztf-16* also has roles in glia that may be independent of its gonadal functions. To test this, we generated animals carrying transgenes containing regions of the *ztf-16* promoter fused to *gfp*. A 2.5-kb region immediately adjacent to the *ztf-16* start codon is expressed in hypodermal and other cell types, but not in glia (data not shown). By contrast, a 2-kb region further upstream (Figure 7A) gives strong, specific expression in AMsh and PHsh glia, in AMso and PHso socket glia, and in an unidentified pair of neurons in the head (Figure 7B). Consistent with this expression pattern, cosmid F43C9, which includes all *ztf-16*-coding fragments but only 300 bp of upstream regulatory sequences, fails to rescue *ver-1* promoter::*gfp* expression in *ztf-16* (*ns171*) mutants (Figure 6, A and B). Furthermore, *ver-1* expression defects in *ztf-16*(*ns169*) and *ztf-16*(*ns171*) mutants are rescued by expression of either *ztf-16a* or *ztf-16b* cDNAs using the constitutive *F16F9.3* glia-specific promoter (Bacaj *et al.* 2008) (Table 2). Finally, we found that a ZTF-16::GFP fusion protein tightly localizes to AMsh nuclei (Figure 7C; *n* = 50), where it may be poised to regulate transcription. Taken together, these results demonstrate that *ztf-16* functions cell-autonomously to regulate transcription of *ver-1* within glia. These results also suggest that the two carboxy-terminal C2H2 zinc fingers, which are absent in ZTF-16a, are dispensable for regulation of *ver-1* expression.

The *F16F9.3* promoter is active starting at the threefold stage of embryogenesis, well after AMsh glia are born (Bacaj *et al.* 2008). That *F16F9.3* promoter::*ztf-16* cDNA constructs

**Figure 2** Mutations in the *Otx* transcription factor *ttx-1* reduce *ver-1* promoter::*gfp* expression. (A) A schematic of the *ttx-1* gene. Exons are represented by boxes; the start codon (+1) is indicated; and regions encoding the DNA-binding homeodomain are shaded. Mutant *ttx-1* alleles isolated in our screen are shown, and the corresponding amino acid changes are indicated. The asterisk indicates a premature stop mutation. The region of the *ns260* deletion is represented by a solid horizontal line [includes insertion (T)<sub>7</sub>CA(T)<sub>14</sub>]. *ns255* likely represents a rearrangement of the gene, shown by a horizontal dashed line (precise ends unknown), as PCR products using primers covering exons 2–6 are absent, weak, or consist of multiple-sized fragments (data not shown). In addition, *ns255* has the same base substitution as *ns235* and *ns252*, causing amino acid change E230K. The previously described *ttx-1* alleles *p767* and *oy26* are also shown (Hedgecock and Russell 1975; Satterlee *et al.* 2001). (B)

are able to rescue the *ver-1* expression defects of *ztf-16* mutants suggests that the gene is not required for early aspects of glia generation, morphogenesis, or development. Indeed, we were unable to rescue *ztf-16* mutants by expressing *ztf-16* cDNA in AMsh glia using an embryonic glia promoter that is not expressed in later larval and adult stages (Table 2). This

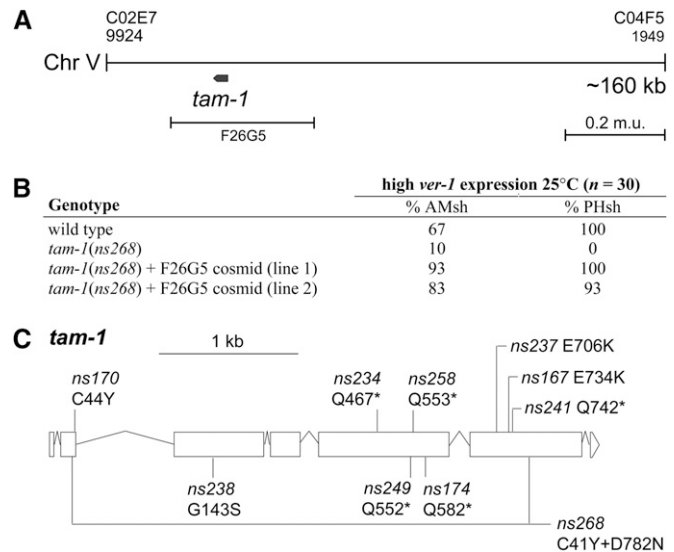


**Figure 3** Mutations in the RING finger and B-box domain factor *tam-1* reduce *ver-1* promoter::*gfp* expression. (A) A schematic of the interval on chromosome V to which the mutant allele *ns258* was mapped. The flanking SNPs are on cosmid C02E7 (base 9924) and C04F5 (base 1949). The regions spanned by the F26G5 cosmid and *tam-1* gene are also shown. (B) Rescue of *ver-1* promoter::*gfp* expression defects of *tam-1*(*ns268*) mutants by two independent extrachromosomal arrays containing the F26G5 cosmid (*nsEx2169* and *nsEx2170*). (C) A schematic of the *tam-1* gene (WormBase release WS225). Exons are represented by boxes. Mutant *tam-1* alleles isolated in our screen are shown, and the corresponding amino acid changes are indicated. Asterisks indicate a premature stop mutation. *ns268* carries two putative amino acid changes.

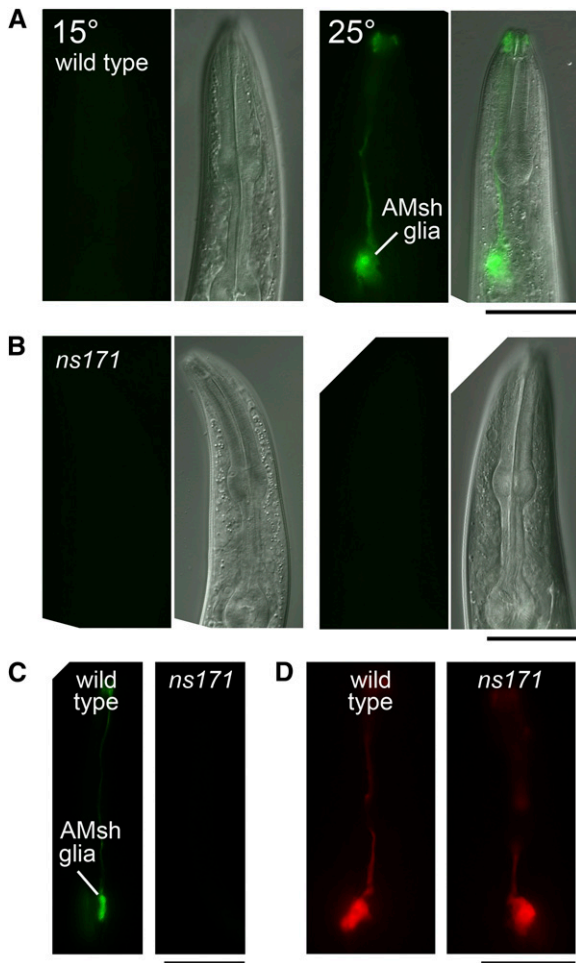


**Figure 4** Temperature- and dauer-induced expression of *ver-1* is reduced in *ns171* mutants. (A) Representative fluorescence images and DIC and fluorescence merged images of *ver-1* promoter::gfp (*nsls22*) expression in one of the two AMsh glial cells of a wild-type adult cultivated at 15° (left) and 25° (right). (B) As in A, except in an *ns171* mutant animal. Exposure time for gfp (A and B), 800 msec. (C) Representative fluorescence images of *ver-1* promoter::gfp (*nsls22*) expression in one of the two AMsh glial cells of a wild-type dauer induced by starvation at 15° (left) and a *ns171* mutant dauer animal (right). Exposure time, 200 msec. (D) Representative fluorescence images of *vap-1* promoter::dsRed (*nsls53*) expression in the AMsh glia of a wild-type adult (left) and a *ns171* mutant adult animal (right). Exposure time, 600 msec. Bar in all images, 50  $\mu$ m. Anterior is up.

embryonic promoter is able to rescue other early AMsh glia defects (Perens and Shaham 2005; Oikonomou *et al.* 2011).

#### ZTF-16 regulates dauer expression of *ver-1* through a site distinct from that bound by TTX-1

We previously showed that robust expression of *ver-1* promoter::gfp transgenes requires residues +1 to +263 of the *ver-1* gene (relative to the ATG start site). We further described a smaller  $\sim$ 90-bp interval sufficient for weak expression of the reporter in glia upon dauer entry. Within this interval, we identified a direct TTX-1-binding site with the core-binding residues located between position +176 and +179 (Procko *et al.* 2011) (Figure 8). Strikingly, we find that the *ztf-16* (*ns171*) mutation reduces *ver-1* reporter expression only if

residues +221 to +263 of the *ver-1* gene are present. Specifically, GFP expression in animals carrying a transgene in which residues +221 to +263 of the *ver-1* promoter are deleted is not altered in *ztf-16* mutants (compare expression in dauers at 25° in wild-type and *ztf-16* animals carrying either the top construct or the second construct from the bottom in Figure 8). Within the region of *ver-1* regulated by *ztf-16*, we identified a potential ZTF-16-binding site, CATGAAAAC, at positions +217 to +225 on the basis of homology to *Drosophila* Hunchback, which binds the consensus sequence (G/C)(C/A) TAAAAA (Stanojevic *et al.* 1989). Mutating these residues to GGGCCCAAC resulted in reduced *ver-1* promoter::gfp expression (compare expression from top and bottom constructs in wild-type adult animals at 25° in Figure 8), raising the possibility that ZTF-16 may bind directly to the *ver-1* gene to regulate its expression. To test for direct binding *in vitro*, we initially attempted to purify soluble full-length GST::ZTF-16a or GST::ZTF-16b protein induced in *E. coli*, but were unable to do so. We were able to purify zinc fingers 2–6 of the protein, but these showed only weak, nonspecific binding to a 40-bp biotin-labeled probe from the *ver-1* gene (data not shown). Thus, it remains unclear whether ZTF-16 directly binds *ver-1*.

Taken together, our promoter studies suggest that ZTF-16 regulates *ver-1* expression directly or indirectly through a site in *ver-1* that is distinct from that used by TTX-1. Our studies also suggest that *ztf-16* does not confer dauer dependence on *ver-1* expression: although *ztf-16* mutants have reduced *ver-1* expression, induction of expression in dauers at 25° is still evident (Figure 8).

Our finding that TTX-1 and ZTF-16 are each required for expression of *ver-1* raised the possibility that these transcription factors require each other to promote AMsh glia-specific expression. To test this idea, we scanned the genome for TTX-1-binding sites similar to that found in *ver-1* (Procko *et al.* 2011) and identified a highly similar sequence (GATTATCG GATTCAG) within a cluster of divergently transcribed genes encoding proteins with thrombospondin domains (Figure S4A). Other proteins with such domains had been previously implicated in glial function in *C. elegans* and in vertebrates (Christopherson *et al.* 2005; Bacaj *et al.* 2008). While a promoter::gfp reporter for one of these genes is expressed exclusively in the AFD neurons, which normally express TTX-1, a similar reporter for another of the divergently transcribed genes of the thrombospondin-domain gene cluster is expressed in AMsh glia (Figure S4, B and C). Expression of the reporter is eliminated in *ttx-1*(p767) mutants (Figure S4D). Importantly, reporter expression was normal in *ztf-16*(*ns171*) mutants ( $n = 53$ ), suggesting that *ttx-1* and *ztf-16* need not function together to promote AMsh gene expression.

#### *ztf-16* function is required in glia for AMsh glia remodeling

Our screen aimed to identify genes controlling the initiation of glia remodeling by identifying regulators of *ver-1* expression. To examine whether *ztf-16* is indeed required for glia remodeling, we used an assay that we previously developed

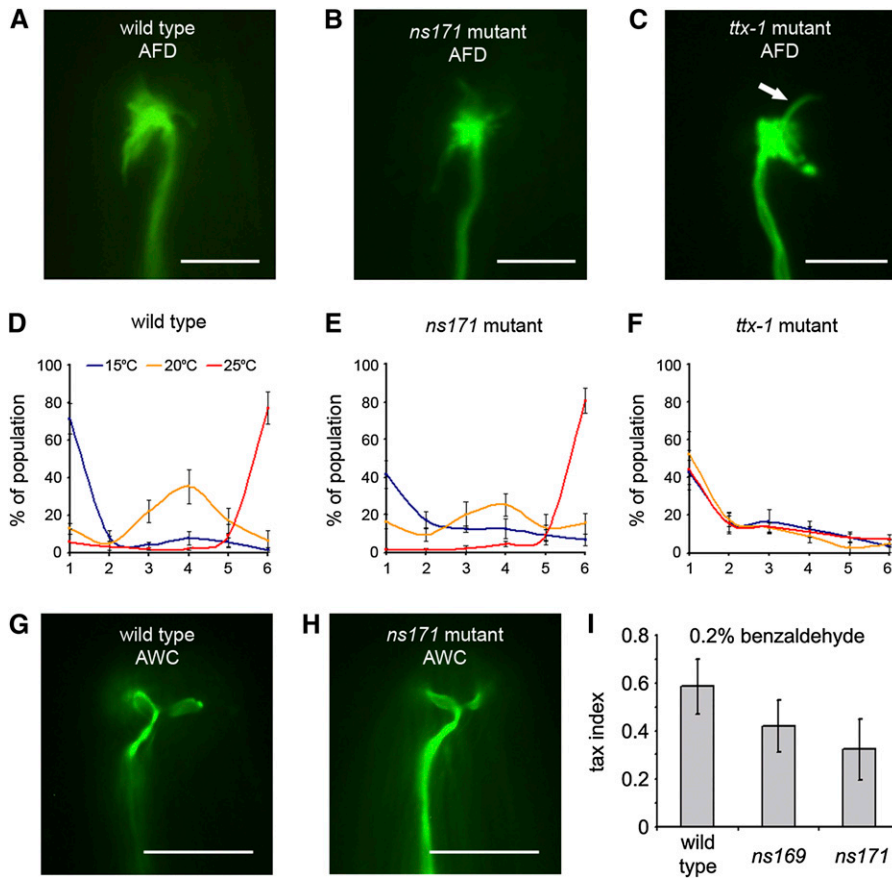


**Figure 5** *ns171* mutants do not strongly perturb sensory neuron morphology or behavior. (A–C) Representative fluorescence images of the AFD dendrite endings of adult wild-type (A), *ns171* mutant (B), and *ttx-1*(*oy26*) mutant (C) strains at 25°. The wild-type microvillar projections are absent or reduced in *ttx-1* mutants, and instead the dendrite terminates in an aberrant, elongated single cilium (arrow in C). Bars, 5  $\mu$ m. Anterior is up. A *gcy-8* promoter::*gfp* transgene (*oyIs17*) was used to visualize the AFD neurons. (D–F) Thermotaxis of wild-type (D), *ns171* mutant (E), and *ttx-1* (*p767*) mutant (F) strains. Animals were cultivated at 15° (blue), 20° (yellow), or 25° (red) prior to performing each assay. The linear temperature gradient is represented by bins 1–6 on the horizontal axis from cold (~18°) to hot (~26°). Wild-type animals migrate to the temperature at which they were cultivated. All values are mean  $\pm$  SD. All animals also carry the *ver-1* promoter::*gfp* transgene (*nsIs22*). F is reproduced from Procko *et al.* (2011). (G and H) Representative fluorescence images of the AWC dendrite endings of L4 wild-type (G) and *ns171* mutant (H) strains. Bars, 5  $\mu$ m. Anterior is up. An *odr-1* promoter::*yfp* transgene (*oyIs45*) was used to visualize the AWC neurons. (I) Chemotaxis index of wild-type and *ns169* and *ns171* mutant adult animals to the AWC-sensed odorant benzaldehyde (0.2%). Values are mean  $\pm$  SD. The difference between *ns169* and wild-type animals is not significant ( $P > 0.05$ ), whereas for *ns171* mutants compared to wild type,  $P = 0.021$  (Student's *t*-test).

to score fusion of the two AMsh glia in dauer animals (Procko *et al.* 2011). Briefly, young *daf-7*(*e1372ts*) mutant larvae cultivated at 25° and harboring an AMsh glia::*gfp* transgene on an unstable extrachromosomal array (*nsEx1391*) were selected for mosaic expression of GFP in one of the two AMsh glia. Mosaic animals were allowed to grow for an additional 48 hr, at which point nearly all became dauers as a result of the *daf-7* mutation. These dauers were then examined for cytoplasmic mixing of GFP between the two glia, which occurs only if the cells have remodeled and fused (Procko *et al.* 2011).

Using this cytoplasmic mixing assay, we found that *ztf-16* (*ns169*); *daf-7*(*e1372*) and *ztf-16*(*ns171*); *daf-7*(*e1372*) dauers had significantly reduced AMsh glia fusion compared to *daf-7* (*e1372*) single-mutant dauers (Figure 9A). Consistent with this result, we found that three of three *ztf-16*(*ns171*); *daf-7* (*e1372*) dauer animals examined by EM failed to exhibit AMsh glia extension and fusion (Figure 9, B and C; Figure S5). We could rescue the fusion defect by restoring *ztf-16* function specifically in glia (Figure 9A). Rescue was more efficient for the *ztf-16*(*ns171*) allele, perhaps because it has a weaker defect than *ztf-16*(*ns169*). Together, these findings suggest that *ztf-16* functions within glia to promote dauer-dependent remodeling.

Our findings that *ver-1* mutants have reduced AMsh glia fusion in dauers (Procko *et al.* 2011) and that *ver-1* expression is greatly reduced in *ztf-16* mutants suggest that, like *ttx-1*, *ztf-16* acts in part to effect remodeling by controlling

*ver-1* expression. We also previously demonstrated a role for the gene *aff-1* in glia fusion (Procko *et al.* 2011). AFF-1 protein functions as a fusogen-promoting syncytium formation in *C. elegans* (Sapir *et al.* 2007). To test whether *ztf-16* might also regulate *aff-1* expression, we examined dauer animals carrying an *aff-1* promoter::*gfp* reporter (*hyEx167*). We found that 95% of wild-type dauers expressed *gfp* in the AMsh glia ( $n = 44$ ) and that 87% of *ztf-16*(*ns171*) mutants expressed *gfp* ( $n = 38$ ). These observations suggest that *ztf-16* is not required for *aff-1* expression.

*ztf-16* may function as a general regulator of AMsh glia morphology or may have specific roles in dauer remodeling. To distinguish between these possibilities, we examined non-dauer *ztf-16* mutant adults carrying a glia-specific *vap-1* promoter::*dsRed* reporter transgene (Figure 4D). We found no gross defects in AMsh glia morphology. Similarly, overall glial shape is normal in electron micrographs of *ztf-16*(*ns171*) mutants. However, in these micrographs, the amphid sensory channel stains abnormally darkly, as do pockets within the AMsh glia (two of three animals examined; Figure S6). Furthermore, some sensory neurons fail to traverse the amphid channel, instead becoming trapped within the AMsh glial cell (Figure S6). These results suggest that, while *ztf-16* may have a general role in proper amphid channel morphology, its function in glial plasticity may be specific to dauer animals, consistent with our findings that *ztf-16* appears to act postembryonically to regulate *ver-1* expression.

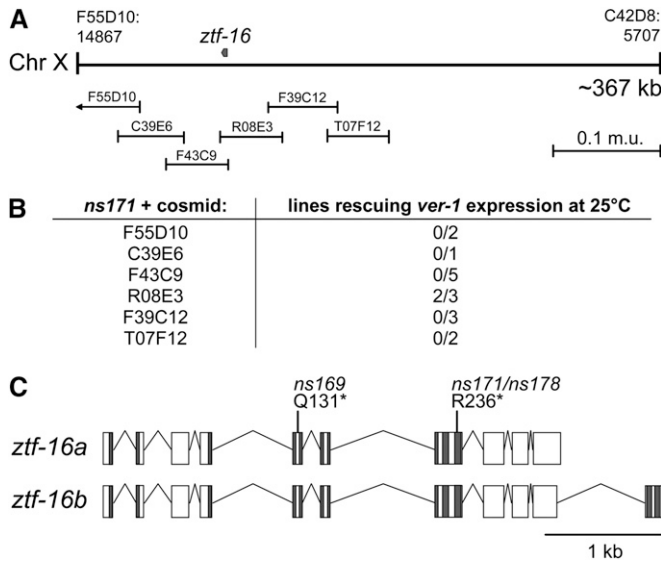


**Figure 6** The C2H2 zinc-finger factor *ztf-16* is required for *ver-1* expression. (A) A schematic of the interval on chromosome X to which mutant allele *ns171* was mapped. The flanking SNPs are on cosmids F55D10 (base 14867) and C42D8 (base 5707). The regions spanned by the cosmids used for the rescue experiments shown in B are indicated, as is the position of the *ztf-16* gene. (B) The number of lines carrying extrachromosomal arrays of the indicated cosmid that rescued the reduced *ver-1* promoter::*gfp* (*nsls22*) expression defect of *ns171* mutant adult animals cultivated at 25°. (C) A schematic of the *ztf-16* gene: exons are boxed; and regions encoding C2H2 zinc-finger domains are shaded. We isolated two splice forms of *ztf-16* on the basis of EST data available from WormBase (release WS225) and have named these gene models *ztf-16a* and *ztf-16b*. The mutant *ztf-16* alleles isolated in our screen are shown, and the corresponding amino acid change is indicated. Asterisks indicate a premature stop mutation.

We previously showed that **AMsh** glia morphological plasticity plays an important role in controlling shape changes of the associated **AWC** sensory neurons (Procko *et al.* 2011). Indeed, in the three *ztf-16* mutant animals that we examined by EM, we found that the **AWC** wing-like cilia that are ensheathed by the **AMsh** glia failed to expand as they normally do in wild-type dauers (Figure 9, B and C). In non-dauer adult or fourth-stage (L4) animals, **AWC** wing morphology is only mildly affected in *ztf-16* mutants as assessed using an *odr-1* promoter::*yfp* reporter (LEtoile and Bargmann 2000). Specifically, 100% of **AWC** neurons of wild-type adults had normal **AWC** wing morphology, while 88 and 83% of *ns171* and *ns169* mutants had normal **AWC** wing morphology, respectively ( $n = 40$  for each strain; Figure 5, G and H). Furthermore, **AWC**-mediated attraction to the odorant benzaldehyde (Bargmann *et al.* 1993) is only somewhat reduced in *ztf-16* mutant adults (Figure 5I). These findings are consistent with the hypothesis that changes in **AMsh** glia influence shape changes of associated **AWC** neurons (Procko *et al.* 2011).

## Discussion

Morphological changes are commonplace for both neurons and glia in the development and homeostasis of the vertebrate

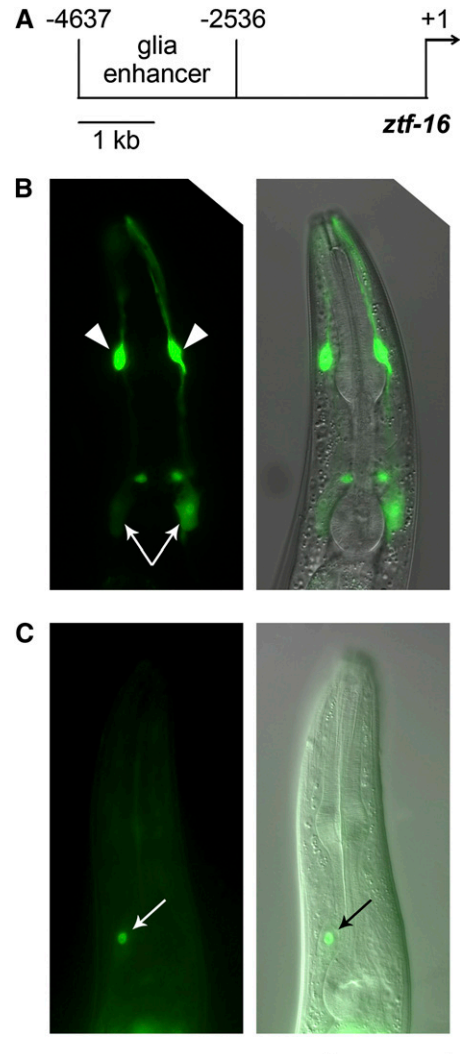


**Figure 7** ZTF-16 is expressed in glia and localizes to the nucleus. (A) A schematic of the *ztf-16* promoter. The start codon (+1) is shown, as well as ~4.6 kb of upstream promoter sequence (solid, horizontal line). The enhancer element used in B is between  $-4637$  and  $-2536$  relative to the +1 start site. (B) Fluorescence image (left) and fluorescence and DIC merged image (right) of an adult animal carrying a transgene containing the *ztf-16* promoter region shown in A driving *gfp* expression (*nsEx3001*). Fluorescence is seen in the two **AMsh** glia (arrows), the **AMso** glia (arrowheads), and a pair of unidentified neurons anterior of the **AMsh** cell bodies. Expression is also observed in the **PHsh** and **PHso** glia in the tail (data not shown). (C) Localization of a ZTF-16::GFP fusion protein to the nucleus of the **AMsh** glia when expressed under a glia-specific promoter (*nsEx1347*). Arrows indicate the **AMsh** glia nucleus. Bar, 50  $\mu\text{m}$ . Anterior is up.

nervous system. How these structural changes in glia are controlled, and whether glial and neuronal shape changes are related, has been largely unexplored. We previously demonstrated that dauer-induced morphological remodeling of the two **AMsh** glial cells of *C. elegans* influences concomitant changes in the glia-ensheathed **AWC** sensory neurons (Procko *et al.* 2011), suggesting that this setting is appropriate for investigating mechanisms and functions of glia remodeling. We showed that glia remodeling depends on the transcription factor *ttx-1* and its direct downstream target, the receptor

**Table 2** *ztf-16* acts in glia to control *ver-1* expression

Genotype <sup>a</sup>	% adult animals expressing <i>ver-1</i> in AMsh glia at:	
	15°	25°
Wild type	0	93
<i>ztf-16(ns171)</i>	0	16
<i>ztf-16(ns171); glia::ztf-16a<sup>b</sup></i>	0	64 <sup>c</sup>
<i>ztf-16(ns171); glia::ztf-16b</i>	0	80 <sup>c</sup>
<i>ztf-16(ns171); embryonic glia::ztf-16b<sup>d</sup></i>	ND	10
<i>ztf-16(ns169)</i>	0	4
<i>ztf-16(ns169); glia::ztf-16a</i>	0	44 <sup>e</sup>
<i>ztf-16(ns169); glia::ztf-16b</i>	0	60 <sup>c</sup>

Transgenes were injected at 60 ng/μl of the rescuing plasmid, with 60 ng/μl of pRF4. Lines shown are *nsEx1389*, *nsEx1410*, *nsEx3266*, *nsEx1382*, and *nsEx1405* and are representative of others. *n* > 25 for all strains. ND, not determined.

<sup>a</sup> All strains contained the *ver-1* promoter::*gfp* transgene (*nsIs22*).

<sup>b</sup> The glia promoter (*F16F9.3*) drives expression in the AMsh and PHsh glia (Bacaj *et al.* 2008). However, rescue of *ver-1* promoter::*gfp* expression in the PHsh glia was not observed (data not shown), perhaps due to low expression levels.

<sup>c</sup> *P* < 0.001. *P*-values were determined using the  $\chi^2$  test. Rescue lines were compared against the corresponding mutant alone.

<sup>d</sup> The glial enhancer element from the *lin-26* promoter (Landmann *et al.* 2004) was used to drive expression in embryonic glial cells.

<sup>e</sup> *P* < 0.01. *P*-values were determined using the  $\chi^2$  test. Rescue lines were compared against the corresponding mutant alone.

tyrosine kinase *ver-1*, whose transcription is induced by dauer entry and high temperature, a dauer stimulus (Procko *et al.* 2011). Here we demonstrate that, in addition to *ttx-1*, the transcription factor *ztf-16* is required for both *ver-1* expression and dauer-induced AMsh glia remodeling. Furthermore, EM analysis of dauer animals suggests that the AWC wing-like cilia fail to take on their expanded overlapping morphology in *ztf-16* mutants, most likely as a result of a failure in glia remodeling. Our results are consistent with a model whereby the transcriptional regulators TTX-1 and ZTF-16 act independently through distinct binding sites to regulate *ver-1* and perhaps other genes required for AMsh glia remodeling.

How might *ztf-16* function be regulated? *ztf-16* was recently shown to interact with the Nemo-like kinase LIT-1 in a yeast two-hybrid assay (Oikonomou *et al.* 2011). Intrigu-

ingly, *lit-1* expression is strongly induced in dauers by the DAF-12 nuclear hormone receptor, which integrates dauer neuroendocrine signals to promote dauer entry (Shostak *et al.* 2004). Furthermore, *ztf-16* mutants possess similar defects in AMsh glial compartment morphology to those of *lit-1* mutants (Oikonomou *et al.* 2011). These observations raise the possibility that LIT-1 kinase may control ZTF-16 function in amphid glia. However, we found that two different alleles of *lit-1* had no defects in *ver-1* promoter::*gfp* expression (data not shown), suggesting that LIT-1 is unlikely to control ZTF-16 function in this context. Nonetheless, AMsh glia remodeling requires membrane growth and is therefore likely mediated by extensive changes in the glial cytoskeleton. LIT-1 was proposed to regulate embryonic aspects of AMsh morphogenesis through physical interactions with the Wiskott–Aldrich Syndrome Protein and actin (Oikonomou *et al.* 2011). Thus, it is possible that LIT-1 and ZTF-16 function together in processes distinct from *ver-1* expression to control glial remodeling.

If ZTF-16 does physically interact with other factors, it is possible that these interactions occur via the two amino-terminal or two carboxy-terminal C2H2 zinc-finger domains, which are unlikely to be required for DNA binding (Large and Mathies 2010). Indeed, the carboxy-terminal zinc fingers of the related Ikaros transcription factor enable dimerization of the protein (Sun *et al.* 1996). However, in our *ver-1* expression rescue studies, we found that the carboxy-terminal zinc fingers are dispensable for *ztf-16* function. Nonetheless, different ZTF-16 isoforms may fine-tune ZTF-16 activity, as is the case for Ikaros, whose activity can be controlled by dimerization with nonfunctional isoforms of the protein (Sun *et al.* 1996).

What other genes control glia remodeling? Most of the mutations that we identified in our screen were alleles of one of three different genes, *ztf-16*, *ttx-1*, or *tam-1*, suggesting that the screen was close to saturation. However, our screen selected for genes involved in controlling *ver-1* expression at high temperatures, and not for genes specifically

<b><i>ver-1</i> promoter fragment fused to <i>gfp</i>:</b>	% animals with AMsh glia GFP expression ( <i>n</i> > 25):					
	wild type				<i>ztf-16</i> mutants	
	adult 15°C	adult 25°C	dauer 15°C	dauer 25°C	adult 25°C	dauer 25°C
	0	93	100	100	16	60 ( <i>P</i> < 0.001)
	0	100	100	100	n.d.	n.d.
	0	0	0	63	0	0 ( <i>P</i> < 0.001)
	0	0	0	63	18	76 (n.s.)
	0	0	n.d.	n.d.	0	n.d.

2011) and the Hunchback (Hb)-related binding site are shown. The asterisk indicates a mutated site (see Results). To test if *ztf-16* was required for expression of a particular reporter, the reporter was crossed to *ztf-16(ns171)* mutants. *P*-values of reporter expression in the *ztf-16* mutant dauers at 25° were determined by comparing the mutant strain against wild type using a  $\chi^2$  test. The integrated transgenes and extrachromosomal arrays used were, from top to bottom, *nsIs22*, *nsEx1136*, *nsEx2174*, *nsEx1269*, and *nsEx3022*. Arrays are representative of others. n.d., not determined; n.s., not significant.

**Figure 8** ZTF-16 regulates expression from the *ver-1* promoter through a site independent of the TTX-1-binding site. The indicated *ver-1* promoter fragments (left, boxes) were fused to a *gfp* fluorescent reporter and tested for expression in the AMsh glia in adults raised at 15° and 25° and in dauers induced by starvation at 15° and 25°. The *ver-1* gene fragments used are indicated relative to the +1 start codon. The *ver-1* promoter::*gfp* transgene used for the mutant screen (*nsIs22*) is shown at the top (~2 kb of upstream promoter sequence through +263 of the *ver-1* gene). The positions of the TTX-1-binding site (Procko *et al.*

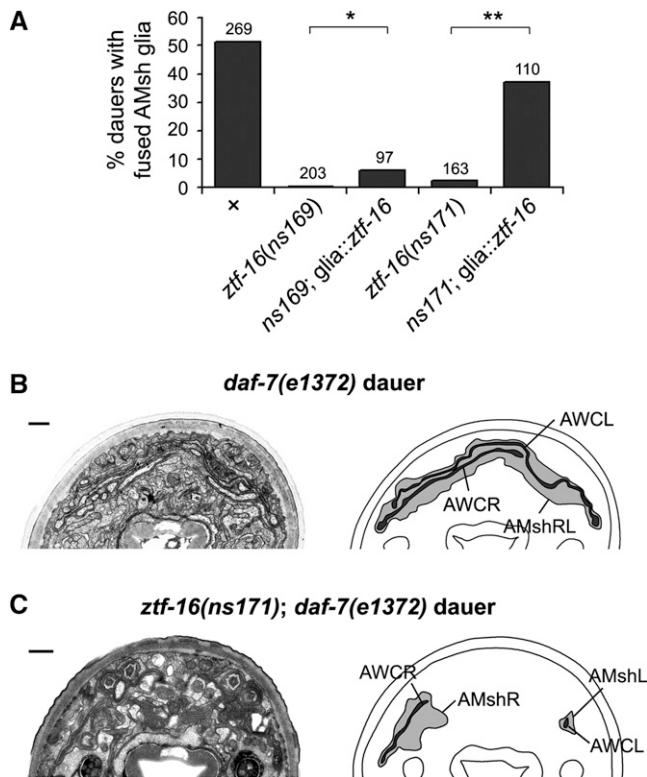


**Figure 9** *ztf-16* function is required for AMsh glial remodeling in dauer animals. (A) Percentage of *daf-7(e1372)* dauer animals of the indicated genotype with fused AMsh glia as scored by cytoplasmic mixing (see Procko *et al.* 2011). Number of animals (*n*) is shown above each column. \**P* = 0.001 (Fisher's exact test); \*\**P* < 0.001 ( $\chi^2$  test). The *glia::ztf-16* transgene is *nsls245* (*T02B11.3* promoter::*ztf-16b*). (B and C) Representative electron micrographs (left) and schematic outlines (right) of the amphid sensory organs of a *daf-7(e1372)* dauer (B) and a *ztf-16(ns171); daf-7(e1372)* dauer (C) cultivated at 25°. Left and right AWC neuron sensory cilia (AWCL/R; dark shading) and AMsh glia (AMshL/R; light shading) are indicated. In C, a section close to the anterior tip of the glial processes is shown where maximum AWC expansion occurs. AMsh glial fusion can occur on either the dorsal or the ventral side of the animal; for simplicity, only the top dorsal half is shown. Bar, 5  $\mu$ m. Dorsal is up. B is reproduced from Procko *et al.* (2011).

required for dauer induction of *ver-1*. Indeed, it remains unclear how dauer signals that induce *ver-1* transcription are perceived by the AMsh glia. These signals may be direct neuroendocrine signals from amphid sensory neurons [e.g., the TGF- $\beta$  ligand DAF-7 (Ren *et al.* 1996)], secondary signals induced as a result of dauer entry (e.g., radial shrinkage of the body circumference), or environmental signals perceived directly by the glia. It is possible that mutant screens assessing *ver-1* expression specifically in dauer animals, rather than in non-dauer adults, may uncover these signals. Direct assessment of glial remodeling, rather than reliance on *ver-1* expression as a proxy, may reveal additional components functioning in parallel to or downstream of *ver-1* to promote glial plasticity.

## Acknowledgments

We thank P. Sengupta and B. Podbilewicz for strains. Other strains used in this study were provided by the *Caenorhab-*

*ditis* Genetics Center, which is supported by the National Institutes of Health (NIH). A. Fire, C. Popovici, and R. Roubin provided plasmids and A. Singhvi provided the image of *ttx-1* mutants. This work was supported by NIH grants R01NS073121, R01HD052677, and R01NS064273 to S.S.

## Literature Cited

- Albert, P. S., and D. L. Riddle, 1983 Developmental alterations in sensory neuroanatomy of the *Caenorhabditis elegans* dauer larva. *J. Comp. Neurol.* 219: 461–481.
- Bacaj, T., M. Tevlin, Y. Lu, and S. Shaham, 2008 Glia are essential for sensory organ function in *C. elegans*. *Science* 322: 744–747.
- Bargmann, C. I., E. Hartwig, and H. R. Horvitz, 1993 Odorant-selective genes and neurons mediate olfaction in *C. elegans*. *Cell* 74: 515–527.
- Brenner, S., 1974 The genetics of *Caenorhabditis elegans*. *Genetics* 77: 71–94.
- Carmona, M. A., K. K. Murai, L. Wang, A. J. Roberts, and E. B. Pasquale, 2009 Glial ephrin-A3 regulates hippocampal dendritic spine morphology and glutamate transport. *Proc. Natl. Acad. Sci. USA* 106: 12524–12529.
- Cassada, R. C., and R. L. Russell, 1975 The dauer larva, a post-embryonic developmental variant of the nematode *Caenorhabditis elegans*. *Dev. Biol.* 46: 326–342.
- Christopherson, K. S., E. M. Ullian, C. C. Stokes, C. E. Mullowney, J. W. Hell *et al.*, 2005 Thrombospondins are astrocyte-secreted proteins that promote CNS synaptogenesis. *Cell* 120: 421–433.
- Dunaevsky, A., A. Tashiro, A. Majewska, C. Mason, and R. Yuste, 1999 Developmental regulation of spine motility in the mammalian central nervous system. *Proc. Natl. Acad. Sci. USA* 96: 13438–13443.
- Golden, J. W., and D. L. Riddle, 1984 The *Caenorhabditis elegans* dauer larva: developmental effects of pheromone, food, and temperature. *Dev. Biol.* 102: 368–378.
- Hedgecock, E. M., and R. L. Russell, 1975 Normal and mutant thermotaxis in the nematode *Caenorhabditis elegans*. *Proc. Natl. Acad. Sci. USA* 72: 4061–4065.
- Hsieh, J., J. Liu, S. A. Kostas, C. Chang, P. W. Sternberg *et al.*, 1999 The RING finger/B-box factor TAM-1 and a retinoblastoma-like protein LIN-35 modulate context-dependent gene silencing in *Caenorhabditis elegans*. *Genes Dev.* 13: 2958–2970.
- Iuchi, S., 2001 Three classes of C2H2 zinc finger proteins. *Cell. Mol. Life Sci.* 58: 625–635.
- Landmann, F., S. Quintin, and M. Labouesse, 2004 Multiple regulatory elements with spatially and temporally distinct activities control the expression of the epithelial differentiation gene *lin-26* in *C. elegans*. *Dev. Biol.* 265: 478–490.
- Large, E. E., and L. D. Mathies, 2010 hunchback and Ikaros-like zinc finger genes control reproductive system development in *Caenorhabditis elegans*. *Dev. Biol.* 339: 51–64.
- Étoile, N. D., and C. I. Bargmann, 2000 Olfaction and odor discrimination are mediated by the *C. elegans* guanylyl cyclase ODR-1. *Neuron* 25: 575–586.
- Lippman, J. J., T. Lordkipanidze, M. E. Buell, S. O. Yoon, and A. Dunaevsky, 2008 Morphogenesis and regulation of Bergmann glial processes during Purkinje cell dendritic spine ensheathment and synaptogenesis. *Glia* 56: 1463–1477.
- Lundquist, E. A., P. W. Reddien, E. Hartwig, H. R. Horvitz, and C. I. Bargmann, 2001 Three *C. elegans* Rac proteins and several alternative Rac regulators control axon guidance, cell migration and apoptotic cell phagocytosis. *Development* 128: 4475–4488.
- McCarty, A. S., G. Kleiger, D. Eisenberg, and S. T. Smale, 2003 Selective dimerization of a C2H2 zinc finger subfamily. *Mol. Cell* 11: 459–470.

- Mello, C., and A. Fire, 1995 DNA transformation. *Methods Cell Biol.* 48: 451–482.
- Mello, C. C., J. M. Kramer, D. Stinchcomb, and V. Ambros, 1991 Efficient gene transfer in *C. elegans*: extrachromosomal maintenance and integration of transforming sequences. *EMBO J.* 10: 3959–3970.
- Meyer-Franke, A., M. R. Kaplan, F. W. Pfrieger, and B. A. Barres, 1995 Characterization of the signaling interactions that promote the survival and growth of developing retinal ganglion cells in culture. *Neuron* 15: 805–819.
- Molnar, A., and K. Georgopoulos, 1994 The Ikaros gene encodes a family of functionally diverse zinc finger DNA-binding proteins. *Mol. Cell. Biol.* 14: 8292–8303.
- Mukhopadhyay, S., Y. Lu, S. Shaham, and P. Sengupta, 2008 Sensory signaling-dependent remodeling of olfactory cilia architecture in *C. elegans*. *Dev. Cell* 14: 762–774.
- Oikonomou, G., E. A. Perens, Y. Lu, S. Watanabe, E. M. Jorgensen *et al.*, 2011 Opposing activities of LIT-1/NLK and DAF-6/patched-related direct sensory compartment morphogenesis in *C. elegans*. *PLoS Biol.* 9: e1001121.
- Perens, E. A., and S. Shaham, 2005 *C. elegans daf-6* encodes a patched-related protein required for lumen formation. *Dev. Cell* 8: 893–906.
- Porter, J. T., and K. D. McCarthy, 1996 Hippocampal astrocytes in situ respond to glutamate released from synaptic terminals. *J. Neurosci.* 16: 5073–5081.
- Procko, C., and S. Shaham, 2010 Assisted morphogenesis: glial control of dendrite shapes. *Curr. Opin. Cell Biol.* 22: 560–565.
- Procko, C., Y. Lu, and S. Shaham, 2011 Glia delimit shape changes of sensory neuron receptive endings in *C. elegans*. *Development* 138: 1371–1381.
- Ren, P., C. S. Lim, R. Johnsen, P. S. Albert, D. Pilgrim *et al.*, 1996 Control of *C. elegans* larval development by neuronal expression of a TGF-beta homolog. *Science* 274: 1389–1391.
- Sapir, A., J. Choi, E. Leikina, O. Avinoam, C. Valansi *et al.*, 2007 AFF-1, a FOS-1-regulated fusogen, mediates fusion of the anchor cell in *C. elegans*. *Dev. Cell* 12: 683–698.
- Satterlee, J. S., H. Sasakura, A. Kuhara, M. Berkeley, I. Mori *et al.*, 2001 Specification of thermosensory neuron fate in *C. elegans* requires *ttx-1*, a homolog of *otd/Otx*. *Neuron* 31: 943–956.
- Shostak, Y., M. R. Van Gilst, A. Antebi, and K. R. Yamamoto, 2004 Identification of *C. elegans* DAF-12-binding sites, response elements, and target genes. *Genes Dev.* 18: 2529–2544.
- Smale, S. T., and K. Dorshkind, 2006 Hematopoiesis flies high with Ikaros. *Nat. Immunol.* 7: 367–369.
- Stanojevic, D., T. Hoey, and M. Levine, 1989 Sequence-specific DNA-binding activities of the gap proteins encoded by *hunchback* and *Kruppel* in *Drosophila*. *Nature* 341: 331–335.
- Sun, L., A. Liu, and K. Georgopoulos, 1996 Zinc finger-mediated protein interactions modulate Ikaros activity, a molecular control of lymphocyte development. *EMBO J.* 15: 5358–5369.
- Tautz, D., R. Lehmann, H. Schnurch, R. Schuh, E. Seifert *et al.*, 1987 Finger protein of novel structure encoded by *hunchback*, a second member of the gap class of *Drosophila* segmentation genes. *Nature* 327: 383–389.
- Theodosis, D. T., and D. A. Poulain, 1993 Activity-dependent neuronal-glia and synaptic plasticity in the adult mammalian hypothalamus. *Neuroscience* 57: 501–535.
- Trachtenberg, J. T., B. E. Chen, G. W. Knott, G. Feng, J. R. Sanes *et al.*, 2002 Long-term in vivo imaging of experience-dependent synaptic plasticity in adult cortex. *Nature* 420: 788–794.
- Ward, S., N. Thomson, J. G. White, and S. Brenner, 1975 Electron microscopical reconstruction of the anterior sensory anatomy of the nematode *Caenorhabditis elegans*. *J. Comp. Neurol.* 160: 313–337.
- White, J. G., E. Southgate, J. N. Thomson, and S. Brenner, 1986 The structure of the nervous system of the nematode *Caenorhabditis elegans*. *Philos. Trans. R. Soc. Lond. B Biol. Sci.* 314: 1–340.
- Wicks, S. R., R. T. Yeh, W. R. Gish, R. H. Waterston, and R. H. Plasterk, 2001 Rapid gene mapping in *Caenorhabditis elegans* using a high density polymorphism map. *Nat. Genet.* 28: 160–164.
- Woolley, C. S., E. Gould, M. Frankfurt, and B. S. McEwen, 1990 Naturally occurring fluctuation in dendritic spine density on adult hippocampal pyramidal neurons. *J. Neurosci.* 10: 4035–4039.
- Yoshimura, S., J. I. Murray, Y. Lu, R. H. Waterston, and S. Shaham, 2008 *mls-2* and *vab-3* control glia development, *hlh-17/Olig* expression and glia-dependent neurite extension in *C. elegans*. *Development* 135: 2263–2275.

Communicating editor: M. Nonet

# GENETICS

Supporting Information

<http://www.genetics.org/content/suppl/2012/01/31/genetics.111.137786.DC1>

## **Sensory Organ Remodeling in *Caenorhabditis elegans* Requires the Zinc-Finger Protein ZTF-16**

Carl Procko, Yun Lu, and Shai Shaham

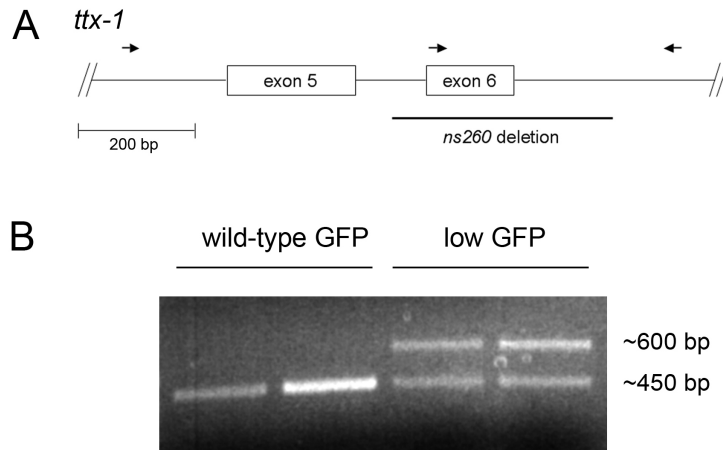


**Figure S1** PCR assay for genotyping *ttx-1(ns260)* animals. (A) Schematic of the *ttx-1* gene, showing only exons 5 and 6 (boxes). The *ns260* deletion is marked. The location of the three oligonucleotide primers used to genotype individual animals (B) are indicated by arrows (5' to 3'). (B) Genotyping of four individual progeny from an *ns260/+* heterozygous parent grown at 25° and carrying a *ver-1* promoter::*gfp* transgene (*nsIs22*). Two of these animals had wild-type levels of *gfp* expression, and had a wild-type genotype (left), while the other two had low levels of *gfp* and were *ns260/+* heterozygous (right). Primers used in the PCR assay are shown in A. Wild-type animals exhibit a single amplified DNA fragment of ~450 bp. *ns260* homozygous animals are predicted to produce only a single DNA band of size ~600 bp.

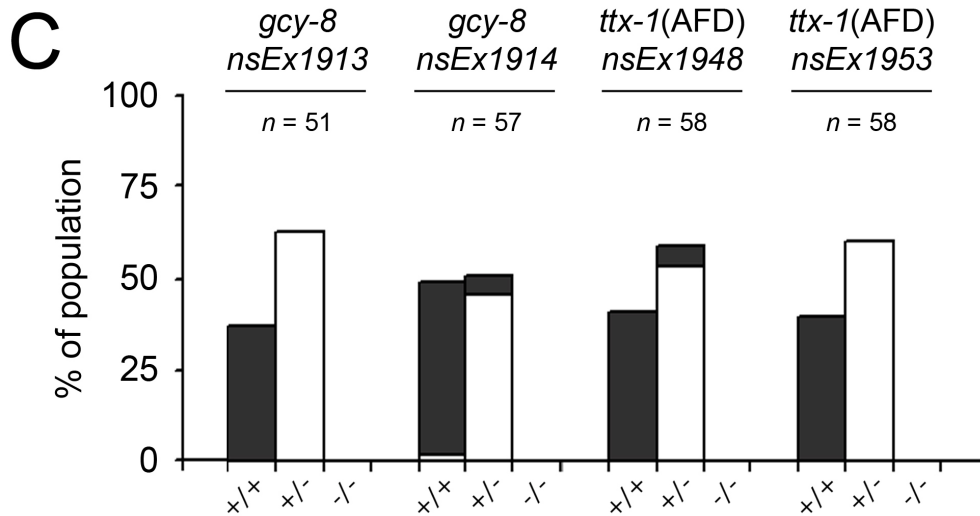
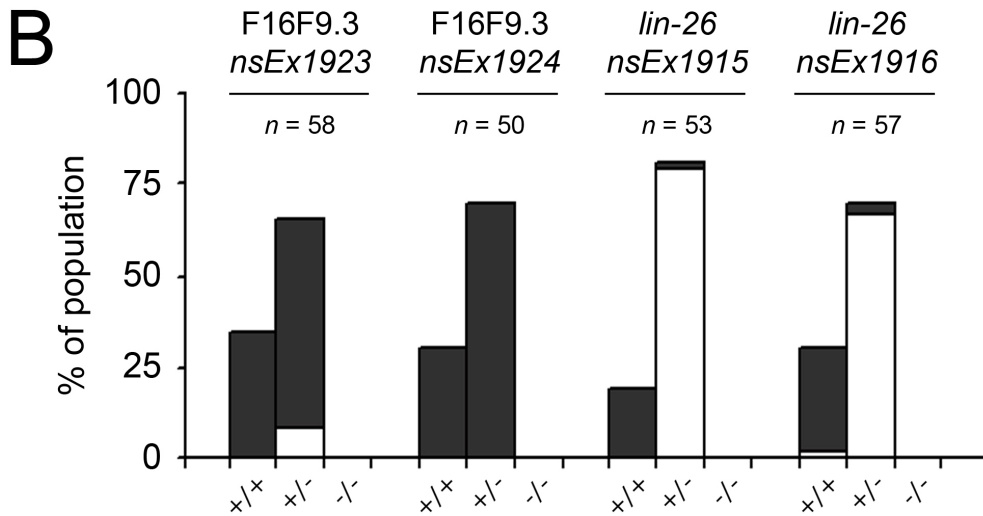
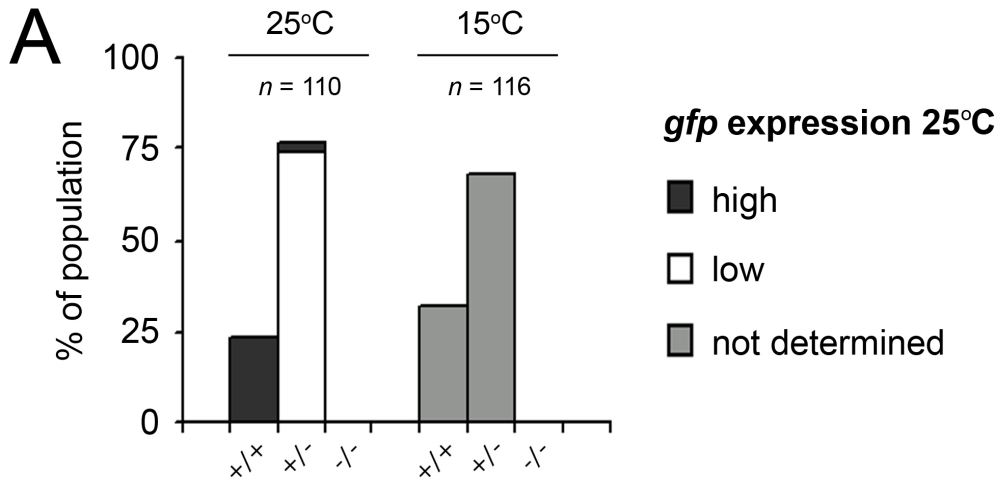


**Figure S2** Glial or AFD-specific expression of *ttx-1* cDNA fails to rescue *ns260* lethality. (A) Genotyping of viable progeny from *ns260/+* heterozygous parents grown at either 15° or 25°. Wild type, +/+; *ns260* heterozygous, +/-; and *ns260* homozygous, -/-. All animals also carry a *ver-1* promoter::*gfp* transgene (*nsIs22*), and levels of *gfp* expression in the sheath glia in each individual animal were scored as either high, low, or not determined. The number of progeny examined (*n*) is indicated. (B) Same as A, except the progeny also carry extrachromosomal arrays restoring *ttx-1* expression in the AMsh glia. Cell-specific promoters driving *ttx-1* cDNA include the *F16F9.3* promoter (late embryo to adult expression (Bacaj *et al.* 2008)) and the *lin-26* promoter (embryonic expression only (Landmann *et al.* 2004)). Two different rescuing arrays using each promoter were scored, and are indicated. The qualitative expression level of *ver-1* promoter::*gfp* at 25° is shown (see legend part A). (C) Same as B, except using AFD-specific *gcy-8* and *ttx-1* promoters. In B and C, the *ttx-1a* splice form was used. In all lines shown in A, B, and C, viable *ns260* homozygous animals (-/-) were never observed.



**Figure S3** *ns171* mutants have wild-type AFD sensory ending morphology. Electron micrograph (EM) showing a cross-section through an amphid sensory organ of an *ns171* mutant adult animal. AFD microvillar projections, red shading. See also Figure 5, A and B. Scale bar, 1  $\mu\text{m}$ . For comparison, see (Ward *et al.* 1975).

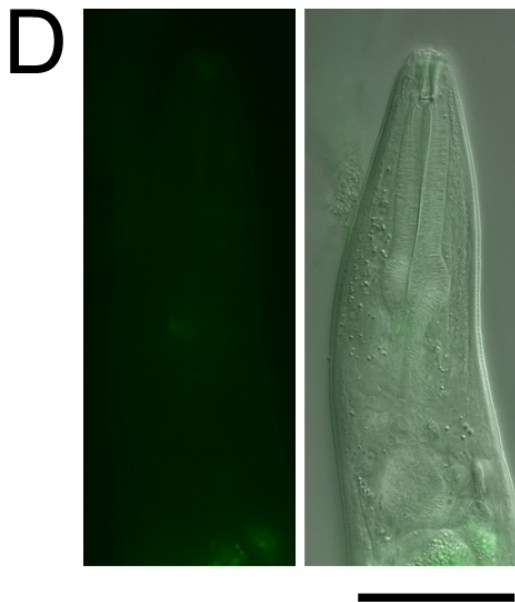
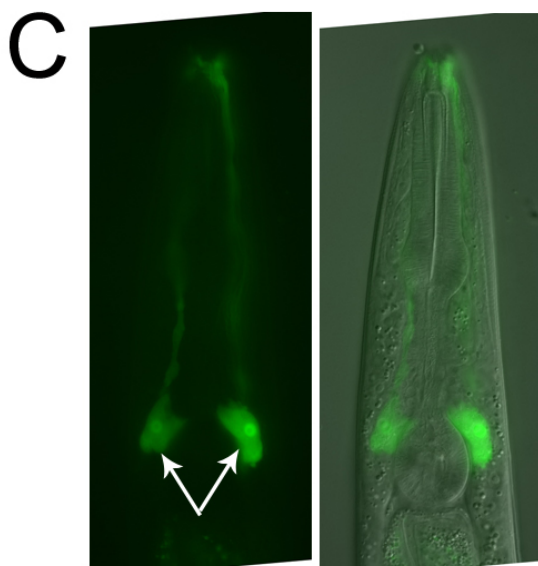
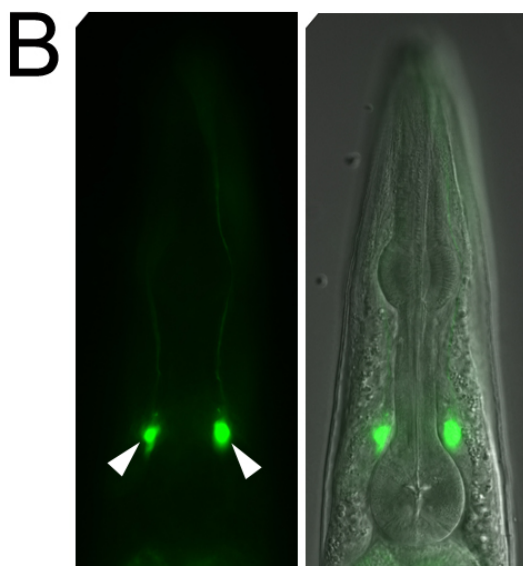
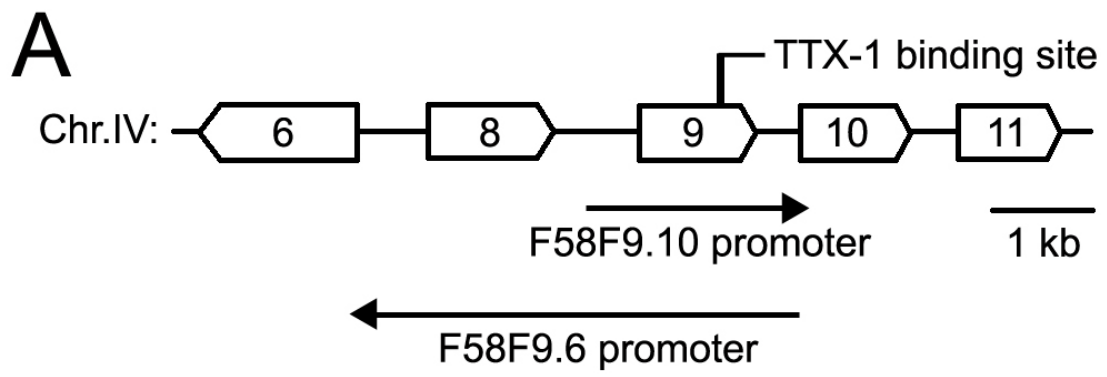


**Figure S4** TTX-1 directly regulates glial and AFD genes. (A) A schematic showing part of the F58F9 cosmid sequence, which includes a cluster of five thrombospondin (TSP)-domain containing genes (boxes). The gene numbers are designated by WormBase. The putative TTX-1 binding site, based on conservation with the *ver-1* promoter, is indicated (conserved residues between *ver-1* and F58F9 are 5' GATTATCGGATTCAG 3', with core TTX-1 binding residues underlined). Also shown are the *F58F9.10* and *F58F9.6* promoter regions used in expression studies. (B and C) Fluorescence images (left), and DIC and fluorescence merged images (right) showing *gfp* expression in the AFD neurons of an adult wild-type animal carrying an *F58F9.10* promoter::*gfp* transgene (*nsEx2284*) (B), or in the AMsh glia of a wild-type animal carrying an *F58F9.6* promoter::*gfp* transgene (*nsEx2330*) (C). GFP expression in AFD is indicated by arrowheads, and in AMsh glia by arrows. Expression of *F58F9.6* promoter::*gfp* in AMsh glia was rare (1/13 lines). (D) As in (C), except in a *ttx-1(p767)* mutant. Exposure (C and D), 500 ms. Scale bar (B-D), 50  $\mu$ m. Anterior is up. All animals grown at 25°C.

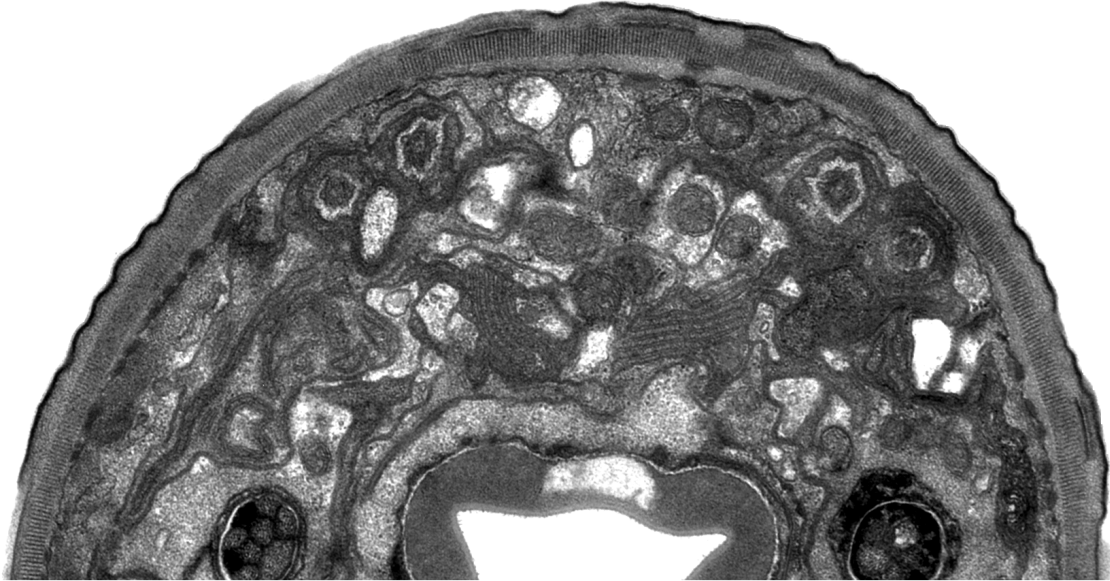


**Figure S5** High resolution image of Figure 9C.



**Figure S6** Electron micrograph (EM) showing a cross-section through the amphid sensory channel of a *ztf-16(ns171)* mutant adult animal. In 2/3 animals examined, the amphid sensory channel (arrow, blue shading) stained abnormally darkly, as did pockets within the AMsh glia (asterisks). Some sensory neurons (red shading) failed to traverse the channel, and were trapped inside the AMsh glial cell (arrowheads). Scale bar, 600 nm. For comparison, see (Ward *et al.* 1975).